HapSense: A Soft Haptic I/O Device with Uninterrupted Dual Functionalities of Force Sensing and Vibrotactile Actuation

Sang Ho Yoon[1*], **Siyuan Ma**[1*], **Woo Suk Lee**[1], **Shantanu Thakurdesai**[1],
Di Sun[1,2**], **Flávio P. Ribeiro**[1], **and James D. Holbery**[1]
[1]Applied Sciences Group, Microsoft, Redmond, WA, USA
[2]Department of Electrical & Computer Engineering, University of Washington, Seattle, WA, USA
{sayoon, siyma, woolee, flaviopr, jiholb}@microsoft.com,
thakurdesai.shantanu@gmail.com, dxs535@uw.edu

ABSTRACT
We present *HapSense*, a single-volume soft haptic I/O device with uninterrupted dual functionalities of force sensing and vibrotactile actuation. To achieve both input and output functionalities, we employ a ferroelectric electroactive polymer as core functional material with a multilayer structure design. We introduce a haptic I/O hardware that supports tunable high driving voltage waveform for vibrotactile actuation while in-situ sensing a change in capacitance from contact force. With mechanically soft nature of fabricated structure, *HapSense* can be embedded onto various object surfaces including but not limited to furniture, garments, and the human body. Through a series of experiments and evaluations, we characterized physical properties of *HapSense* and validated the feasibility of using soft haptic I/O with real users. We demonstrated a variety of interaction scenarios using *HapSense*.

Author Keywords
Haptics, Wearables, I/O Device, Soft Actuator, Soft Sensor

CCS Concepts
•**Hardware** → Sensors and actuators; Tactile and hand-based interfaces; •**Human-centered computing** → Haptic devices;

INTRODUCTION
Haptic feedback systems have been widely adopted to efficiently transfer, convey and enhance information from digital interfaces. With emerging interfaces (e.g., augmented/virtual reality and wearables), the role of haptic feedback becomes significantly important because visual attention is distracted away from input devices to either immersive display [6] or everyday activity (e.g., walking, driving) [8]. Among various haptic feedback approaches, vibrotactile mechanism is highly populated for their technical maturity with granted safety [10, 57]. However, most haptic feedback systems still rely on rigid and bulky hardware components which limit applicability in highly flexible system or hinder potentials of seamless device integration.

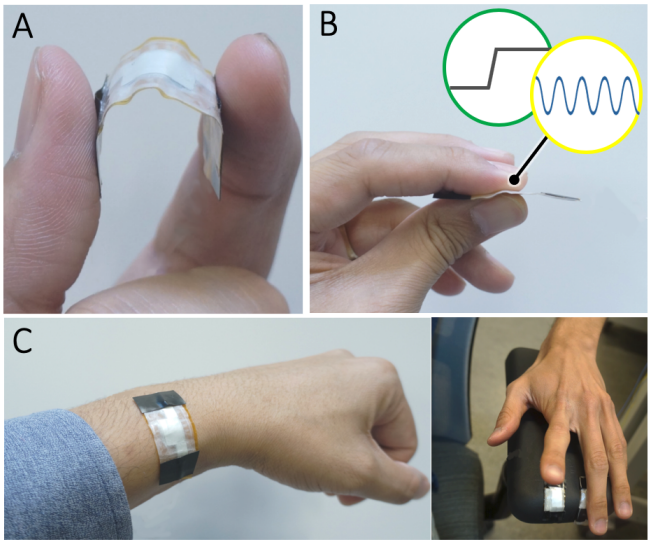

Figure 1: *HapSense* is (A) a soft haptic I/O device that (B) provides uninterrupted force sensing (green circle) and vibrotactile feedback (yellow circle) while working with (C) various objects and surfaces.

To overcome these limitations, researchers have explored I/O devices which are constructed with soft materials to achieve sensing [61] and haptic actuation [63]. With soft materials, researchers have accommodated requirements of high flexibility, low-profile, and comfort [34]. Still, it is challenging to employ these devices for general user interaction purposes because of a safety concern resulted from high operating voltages (>1 kV) [33]. In this work, we chose PVDF ferroelectric polymer materials as core functional component which are mechanically soft and requiring relatively low driving voltage comparing to other soft actuators [47]. By employing a multilayer structure, we achieved driving voltage less than 300 V for perceptible actuation.

[*] The first two authors contributed equally to this work.
[**] Work done while the author was at Microsoft.

UIST '19, October 20-23, 2019, New Orleans, LA, USA.

ACM ISBN 978-1-4503-6816-2/19/10 ...$15.00.
http://dx.doi.org/10.1145/3332165.3347888

Previously, coordinating sensing and actuating functionalities showed improvements of user performance for touchscreen interaction [23]. Recent works including tactile display and shape-changing interface have also shown promising results. To ensure high-quality user experience, simultaneous or smooth transition between sensing and actuation functionalities should be achieved to avoid any negative effects due to user-perceptible interruptions [1]. Previous approaches, however, require discrete hardware components to achieve these functionalities due to hardware incompatibility and system integration complexity. Using discrete hardware components for sensing and actuation inevitably increases the overall system complexity, physical size, and manufacturing cost.

In this work, we introduce *HapSense*, a single-volume soft haptic I/O device that provides uninterrupted force sensing and vibrotactile actuation. We utilize a multilayer ferroelectric electroactive polymer to achieve driving voltage less than 300 V. We came up with a miniaturized system that supports concurrent force sensing with controllable vibrotactile feedback. Also, we employed a low-cost fabrication process to support building soft haptic I/O devices in general lab setting. With proposed soft device, *HapSense* can be embedded onto surfaces with various rigidities and geometries. This will enable new opportunities of bringing I/O functionalities by embedding *HapSense* to a wide range of objects and surfaces.

- A single-volume PVDF device enabling uninterrupted sensing and actuation functionalities with a novel control hardware;
- A low-cost soft I/O device fabrication process without need of industrial-scale machinery or prior fabrication experience;
- Analysis of experiments and task evaluations for a soft haptic I/O device;
- Example applications demonstrating the practical use of *HapSense* in various form factors

RELATED WORK

Coordinating Haptic Sensing and Actuation

As haptic feedback becomes widely adopted in various devices and interfaces, researchers have coordinated sensing capability with new types of haptic feedback. Examples include but are not limited to tactile displays [25, 27, 41], shape changing displays [15, 48, 52], close-loop haptic feedback devices [36, 37, 49, 50], and eyes-free wearables [43, 45, 55]. Moreover, integrated tactile feedback used with sensing device has also shown promising performance for user interactions [23]. However, previous works require discrete hardware components to achieve simultaneous actuation and sensing functionality, which results in complicated system design, large overall device size, and increased manufacturing cost. Thus, we aim to build a single-volume haptic I/O device with advanced control hardware and software to enable integrated and uninterrupted haptic sensing and actuation functionalities.

Soft I/O Devices in HCI

Soft I/O devices have shown in HCI applications with good body-conformability and mechanical durability. For input sensing purposes, researchers have developed soft devices with refined sensing capability [42, 62, 65] and on-skin compatibility [11, 30, 61]. On the other hand, researchers have also explored haptic actuation through flexible and soft devices [3, 22, 63, 64]. Although these works have demonstrated promising input or output functionality, systems with simultaneously integrated sensing and actuation functionalities are rarely reported [7]. In this work, we focus on bringing a soft haptic I/O device that delivers simultaneous force sensing and controllable vibrotactile actuations.

Soft & Self-Sensing Actuators

Soft actuators are classified into three types based on material natures. These include electroactive polymer (EAP), twisted and coiled polymer (TCP), and pneumatic-driven artificial muscle (PAM) [2, 9, 20, 40]. Among these types, we focus on EAP since TCP generally shows low power efficiency and PAM requires bulky pneumatic driving system. In terms of EAP, it includes dielectric electroactive polymer actuator (DEA) [19] and ionic electroactive polymer actuator (IEA) [58]. DEA shows a large output force with a rapid response but requiring a high driving voltage (>1 kV). In contrast, IEA requires a low driving voltage but it provides a slow actuation and requires encapsulation to prevent electrolyte loss. We adopted a multilayer ferroelectric EAP which exhibits all the advantages from a DEA and requires no encapsulation or a high driving voltage. This approach entitles advantages over combining discrete sensor and actuator [59] because *HapSense* operates at less power with simpler system control.

Previous studies demonstrated DEA actuators with sensing capability called *self-sensing actuator* [12, 28, 31, 35, 51, 54]. Multilayer stack EAP actuators using P(VDF-TrFE) (Poly vinylidenfluoride-co-trifluoroethylene) copolymers [5, 17, 47] have been studied to support actuation with low driving voltage. However, a PVDF-based device which simultaneously serves as sensor and actuator with uninterrupted dual functionalities is still lacking according to the best of our knowledge. In addition, previous works required discrete physical devices or bulky power supply to operate sensing or actuation. Thus, we propose a novel hardware and system workflow to support force sensing integrated with simultaneous vibrotactile actuation.

DESIGN GOALS AND CHALLENGES

Soft Material: Flexible sensors/actuators become popular with the emerging applications such as VR and gaming. Aligned with this direction, *HapSense* needs to be constructed with soft materials which physically support flexibility and softness. Also, integrating haptic feedback and sensing has been a challenge. Our approach would allow using soft materials as both sensor and actuator. With a low-profile form factor, we expect that our prototype can be deployed as standalone form factor or conformally wrapped onto 3D objects/bodies.

I/O Interaction Methodology: Integrated actuation with sensing capability in a single device can deliver localized haptic feedback triggered by user applied contact force. For example, *HapSense* can provide vibrotactile feedback subsequent to sensing user's physical contact. Being made with

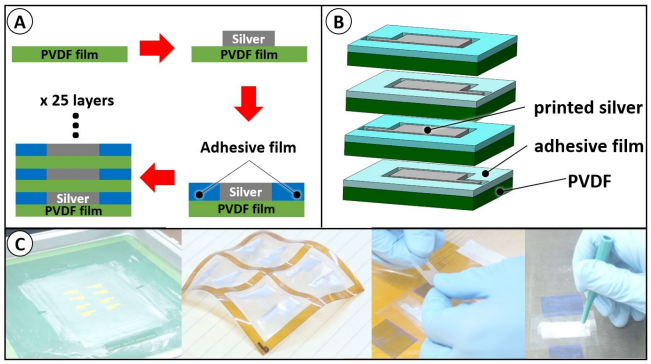

Figure 2: *HapSense* (A) overall assembly process, (B) individual layer construction, and (C) fabrication process (left to right: electrode screen printing, PVDF patterned with electrodes, layer stacking and electrode through-holes punch).

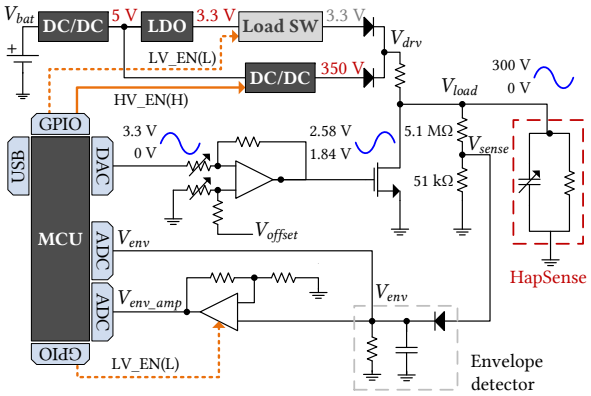

Figure 3: Schematic view of the *HapSense* board.

soft materials, *HapSense* has a potential to deliver vibrotactile signals without shaking rigid mounting structures or generating undesired audible signals. To confirm the feasibility of the aforementioned interaction methods, we need to evaluate and set design parameters for the perception of vibrotactile feedback coordinated by concurrent force sensing.

Fabrication: Fabrication of a soft material device often requires advanced process knowledge or expensive equipment. Also, the fabrication process of the soft material device is often difficult to scale in manufacturing. We aim to enable HCI practitioners to build and deploy their soft I/O device without high cost or exotic equipment. To achieve this, a fabrication process should enable ease of adoption in common lab settings with no special or high-cost equipment requirement.

FABRICATION OF HAPSENSE

The fabrication of *HapSense* consists of 1) patterning the prepared ferroelectric films with a conductive silver electrode using screen printing technique forming individual repeating unit and 2) vertically stacking multiple units using laser-patterned adhesive films resulting a multilayer structure which consists of alternating ferroelectric polymer and electrode layers (Figure 2(A)). Unlike previous soft sensor fabrication works [16, 53], our approach does not require industrial-grade pad printer or pre-stretching process. Only standard lab skill and low-cost equipment like screen printing consumables are needed to fabricate *HapSense*. We fabricated our PVDF film to ensure high film quality (e.g., free of pin holes and defects at thin form factors) using ferroelectric polymer material within a suspension of ketone solvent (**Appendix**), but identical performance can be achieved with commercially available PVDF film [46].

Manual screen printing technique was adopted to form conductive electrode patterns on prepared low-modulus PVDF films (Figure 2 (C)). We used the ink consisted of stretchable silver flake composite (Metalon HPS-021LV, Novacentrix). Our screens were woven stainless-steel threads with 200 mesh density. After screen printing, the printed pattern was cured at 100 °C for 1 hour. Subsequently, 10 μm thick laser patterned acrylate adhesive film (82601, 3M) was manually applied around the silver printed area. The fabricated structure shown so far is defined as a repeating unit. Multiple repeating units (25 layers) were vertically adhered manually with the applied adhesive tape as shown in Figure 2 (B). An electrical connection between alternating electrodes was resulted by applying a conductive epoxy (Ablestik 2030SC, Henkel) to punched 2 mm diameter through-holes on the shared electrode overlapping area. This whole process took about 2 hours including screen printing, curing, and assembly. Finally, the fabricated device attached using adhesive tape (9471 LE, 3M) or wrapped with a thin (<60 μm) plastic sealing tape to ensure uniform and consistent surface contact.

Our fabrication method created a minimum device dimension of 5 mm $\times$ 5 mm $\times$ 0.7 mm with a minimum bending radii of 2 mm. This is limited by manual alignment process of repeating layers. For this study, we devised the device dimension of 35 mm $\times$ 14 mm $\times$ 2 mm with an active area of 12 mm $\times$ 8 mm, close to the size of fingertip. We chose the number of layers greater than 20 to provide greater than 200 mN/cm^2 force feedback with 200 V [47]. Utilizing a 3-point bending test, we characterized the bending stiffness of the proposed device as 15 MPa. We also measured the hardness of *HapSense* (62 Shore A) which is softer than polyethylene naphthalate substrate (67 Shore D) used in [17].

HAPSENSE HAPTIC I/O OPERATING PRINCIPLE

HapSense generates vibrotactile feedback with a time-varying driving voltage across adjacent electrodes. And, it works as a force sensor based on capacitive sensing mechanism. Working as an actuator, PVDF piezoelectric polymer films were deformed once electrical charges are induced. Working as a force sensor, dielectric geometry changes caused by external force results in overall system capacitance change which is interpreted as applied forces. To implement a portable soft haptic I/O system, we designed a battery-operated low-power board capable of generating sufficient voltage (0$\sim$300 V) with arbitrary analog waveform. Also, our system can simultaneously actuate and sense with two operation modes: 1) *hybrid* mode and 2) *sensing-only* mode. The board supports seamless transition between the two modes. We introduce each operation mode in detail and explain the hardware/software architectures that enable these two modes.

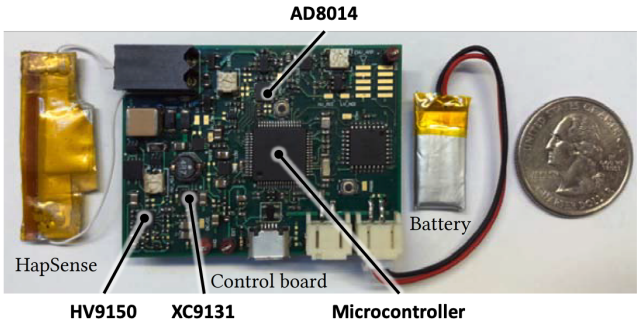

Figure 4: Hardware configured with *HapSense*.

Hybrid & Sensing-only Modes

Hybrid mode refers to measuring forces applied to *HapSense* during device actuation. *HapSense* is a capacitive load that we exploit to achieve simultaneous sensing and actuation functionalities instead of measuring the charge generated from piezoelectric effect. This enables concurrent actuation and force sensing without adding system complexity from accommodating piezoelectric effect. As a function of increased input force, *HapSense* exhibits increased capacitance because of the decreased dielectric layer thickness. The increased capacitive value translates into attenuated magnitude of the voltage waveform applied across *HapSense* electrodes. Therefore, we measure the force level by monitoring the actual voltage across *HapSense* using an envelope detector and subsequent signal processing algorithm. In this mode, we apply input voltage of above 100 V across *HapSense*.

For applications where only sensing functionality is needed, *HapSense* can act as a sole contact force sensor. By adopting the same technique as above, we provide sensing capability with significantly lower voltage (3.3 V). The reduction in driving voltage lowers an overall power consumption under the circumstance when only sensing is required. Supporting both modes using the same hardware lowers system cost, physical size, as well as system complexity.

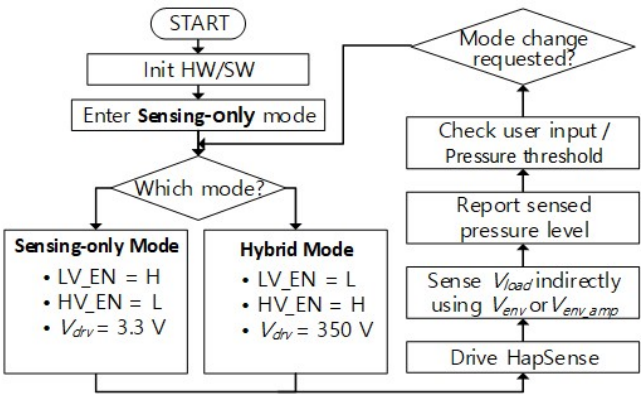

Figure 5: System flow supporting soft haptic I/O.

Operation Mode	V_{bat} (V)	V_{drv} (V)	I_{bat} (mA)	P_{bat} (mW)	High Voltage Generation Overhead (mW)
Hybrid	3.7	350	173	640	348
Sensing-Only	3.7	3.3	79	292	N/A

Table 1: Overall power consumption for two operation modes

HW/SW Implementation

In this section, we introduce the hardware and software architectures of *HapSense* and discuss its system workflow and performance. Figure 3 and 4 illustrate a schematic block diagram and major components of the board, respectively. The block diagram depicts the case where board is configured for the *hybrid* mode.

Hardware Development

The board is powered by a single 3.7V lithium polymer battery. The input voltage is regulated to 5 V using a DC/DC converter IC (XC9131, Torex), which is further used to source a high-voltage DC/DC controller IC (HV9150, Microchip). The 5 V output is further regulated to 3.3 V to supply a control subsystem, MCU (MK20DX256V, NXP). The board employs a common-source MOSFET amplifier circuit to generate a high-voltage (e.g., 350 V) arbitrary analog waveform. We ensure electrical safety during high voltage manipulation by adding discrete hardware verification logic. In order to minimize power consumption, we operate MOSFET amplifier at near threshold.

Due to the high-ratio voltage conversion (i.e., 3.7 V to 350 V), the board is designed to take full advantages of different conversion efficiencies provided by individual regulators. Table 1 summarizes overall system voltage, current, and power consumption for each operation mode driven with 450 Hz sine wave. We measured power consumptions at the battery level to reflect the power consumption of entire system. As shown in Table 1, the *hybrid* mode and the *sensing-only* mode power consumptions are 640 mW and 292 mW, respectively. Given that both modes utilize the same hardware, the power consumption difference is mainly from the high-voltage generation for actuation. The actual power consumed by *HapSense* device itself was found out to be less than 3 mW. Comparing to commercial piezoelectric actuator [59] (5 mW) and conventional motor driver [24] (1480 mW@200 V_{pp}), *HapSense* consumes much less power for the device operation.

System Workflow

The MCU generates a rail-to-rail (i.e., 0 V to 3.3 V) analog driving waveform using digital-to-analog converter. Then, the waveform is attenuated and offset to proper Q-point using a differential opamp where gain is controlled by a digital potentiometer. Depending on the mode controlled by the `HV_EN` and `LV_EN` signals, V_{drv} is either > 100 V or 3.3 V minus forward voltage drop (V_f) of the Schottky diode for the *hybrid* mode and the *sensing-only* mode, respectively.

While *HapSense* is being driven, a proportionally diminished waveform (V_{sense}) mirroring the amplified driving voltage (V_{load}) appears at the mid-junction of a voltage divider. Next, V_{sense} gets fed to a envelope detector that outputs V_{env}, which follows the peak magnitude of V_{sense}. As opposed to the *hybrid*

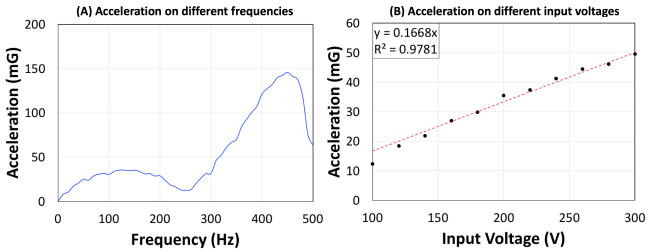

Figure 6: Actuator acceleration characterization: accelerations from various (A) input frequencies and (B) input voltages (with 160 Hz frequency).

mode where V_{env} is sufficiently high enough to be read directly by the analog-to-digital converter (ADC), in the *sensing-only* mode, an op-amp is activated and facilitates the ADC reading by amplifying V_{env} to V_{env_amp}.

TECHNICAL EVALUATION

To understand the *HapSense* structure and performance, we measured *HapSense*'s performance as an actuator (e.g. output force, displacement) and as a sensor (e.g. capacitance change as function of input force). Furthermore, we investigated thermal characteristics of both PVDF ink and cured film, surface morphology, structural thickness, and electrode resistivity which are enclosed in the **Appendix**.

Device performance as an actuator

First, we characterized actuator acceleration using an inertial measurement unit (MPU9250, TDK, JP). The overall test specimen mass (HapSense under test and IMU test board) was 15 g. The PVDF structure shows a broad-band actuating frequency range centered at 160 Hz and 430 Hz (Figure 6(A)). Figure 6(B) shows a relationship between accelerations and different input voltages. From 100 V to 300 V, we observed linear relationship between acceleration and input voltage.

We measured output force and displacement using a MEMS analysis device (Aurora Scientific, CA). A sinusoidal waveform was used as driving signal at various peak voltage values.

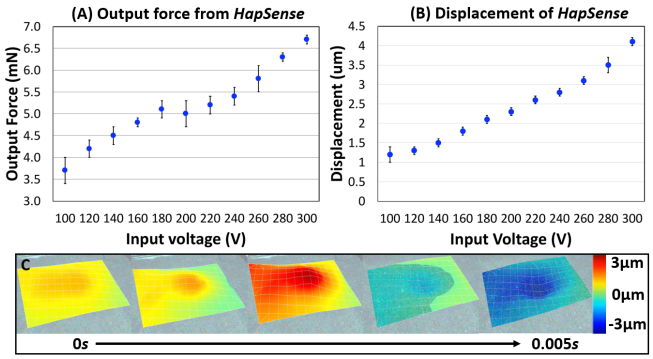

Figure 7: (A) Output force and (B) displacement measurements using a MEMS analysis device. (C) Captured time-revolved motion with using a laser vibrometer.

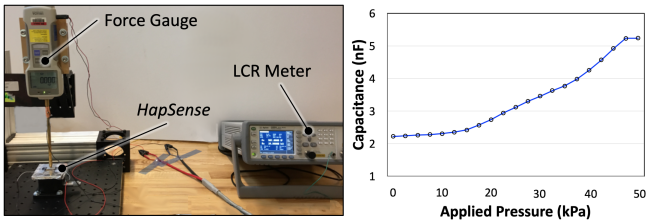

Figure 8: Custom-designed capacitance test measurement system (left) and result of capacitance characterization of *HapSense* as a sensor (right).

From 100 V to 300 V, the actuating output force was continuously modulated from 3.7 mN to 6.7 mN (Figure 7(A)) and force displacement from 1.2 μm to 4.1 μm (Figure 7(B)). These results show that HapSense can fulfill a minimum detection threshold for the hand skin neural receptors where the minimum detection threshold can be as low as 0.16 μm at 250 Hz with a stimulation area of 5cm^2 [29]. In addition, we confirmed displacement of *HapSense* during actuation using a laser vibrometer (Polytech, PSV-500 Scanning Vibrometer). The measured results are consistent with result achieved using the MEMS analysis device. For input voltage, we regulated max input voltage to be less than 400 V due to occasional electrical breakdowns of PVDF layer above 400 V.

Device performance as a sensor

Sensor performance was characterized, as shown in Figure 8, using a custom system consisting of a z-axis stage (Newport), a force gauge (Imada, JP) and an LCR meter (Agilent 4556). The force gauge was fixed at a stationary location while a z-stage was controlled manually for desired displacement value. The force gauge tip has an area of 80 mm^2. Without applying external pressure, system capacitance was measured approximately 2.2 nF. When the applied pressure was increased from 0 kPa to 12 kPa, a minor increase in capacitance was observed fitting equation of $C = 0.0103P + 2.21$. From 12 kPa to 0.45 kPa, a rapid capacitance increase was measured fitting equation of $C = 0.0817P + 1.15$. For the equations above, C is measured capacitance value in nF and P is applied pressure in kilopascal. For pressures larger than 45 kPa, we did not observe apparent capacitance changes.

EXPLORATORY STUDY

For *HapSense*, we investigated following two fundamental questions: 1) What is the minimum driving voltage required to provide tactile sensation above user perception with *HapSense*? 2) What types of actuation driving waveform deliver the preferred user experience and effective performance using *HapSense*? For this study, we recruited 9 participants with a mean age of 30 (4 female) and each participant wore earplugs to avoid biases from any environmental noises during first two studies. We used a prototype made with 25 PVDF layers with an active area of 12 mm $\times$ 8 mm.

Minimum Driving Voltage Threshold for Tactile Sensation

Based on a psychophysical research for tactile design guidelines, the minimum pressure to stimulate fingertip mechanore-

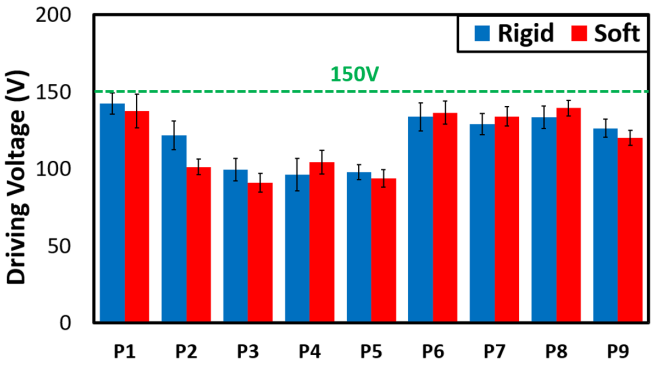

Figure 9: Absolute tactile threshold per participant with recommended minimum driving voltage (150 V).

ceptors needs to be greater than 60∼200 mN/cm^2 [21]. Previous work [47] simulated that more than 20 PVDF-TrFE layers with a driving voltage of 200 V are needed to achieve force greater than 200 mN/cm^2 which led our prototype design with greater than 20 PVDF layers (25 layers in this paper). In this study, we investigate minimum driving voltage of *HapSense* for absolute voltage threshold which results in actuation above user's perception level. This will provide information about proper driving voltage to be used with multilayer PVDF actuators for interaction purpose, which has not been reported in literature according to the best of our knowledge.

Setup: We used a random, double Staircase Method (20 steps per staircase) which is a modern variation based on the Method of Limit [13, 18]. For *HapSense*, the starting stimulus intensity for the descending staircase was 300 V due to dielectric breakdown. Participants maintained their contact with the prototype using the index finger of the dominant hand. In order to avoid any interaction effect from a fatigue, we guided users to rest arms on the table during the study. A minimum stimulus onset asynchrony of 2 s was provided between each step and the threshold was computed by averaging last 10 reversals from each ladder.

We guided and advised users to prevent applying force above 0.6 N by applying a digital scale under the *HapSense* device. This ensures that our investigation is within the scope of tactile sensation with a light touch similar to a user-touch screen

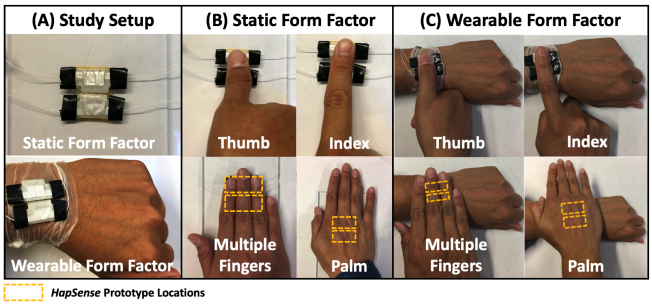

Figure 10: (A) The overall study setup using four different hand regions with (B) static and (C) wearable form factors.

Waveform/ Frequency	Surface	Accuracy (%)		Subjective Response		
		Single	Dynamic	Sensitivity	Comfort	Discernibility
Sine/ 160 Hz	Rigid	92.5 (±11.18)	97.50 (±5.59)	4.0 (4.00-5.00)	**5.0 (5.00-6.25)**	4.50 (4.00-5.25)
	Soft	89.64 (±10.59)	87.98 (±2.21)	4.0 (3.00-5.00)	5.0 (4.75-6.00)	4.0 (3.00-4.00)
Sine/ 430 Hz	Rigid	89.29 (±11.78)	85.00 (±20.54)	4.0 (3.00-6.00)	5.0 (4.00-6.25)	4.5 (3.00-5.00)
	Soft	87.50 (±7.22)	78.33 (±19.18)	3.0 (2.00-4.00)	5.0 (4.00-5.00)	3.0 (2.00-4.00)
Square/ 10 Hz	Rigid	92.50 (±6.85)	**100.00 (±0.00)**	**5.0 (4.75-6.00)**	5.0 (4.00-6.00)	**5.0 (5.00-5.25)**
	Soft	85.00 (±10.46)	93.33 (±6.32)	4.0 (4.00-5.00)	4.5 (4.00-5.00)	4.0 (4.00-5.00)
Square/ 160 Hz	Rigid	**100.00 (±0.00)**	92.50 (±11.18)	**5.0 (5.00-5.25)**	5.0 (5.00-6.00)	4.0 (4.00-5.00)
	Soft	87.50 (±9.32)	90.00 (±16.30)	4.5 (4.00-6.00)	5.0 (5.00-6.00)	4.0 (4.00-5.25)
Sawtooth/ 10 Hz	Rigid	97.50 (±5.59)	**100.00 (±0.00)**	5.0 (4.00-6.00)	5.0 (4.75-6.25)	5.0 (5.00-6.00)
	Soft	89.12 (±10.87)	95.83 (±5.89)	4.0 (3.75-4.25)	5.0 (4.00-5.00)	4.0 (4.00-5.00)
Sawtooth/ 160 Hz	Rigid	92.5 (±6.85)	94.64 (±7.36)	4.5 (3.00-5.25)	5.0 (5.00-6.00)	4.0 (3.75-5.00)
	Soft	83.09 (±13.89)	95.00 (±6.85)	3.5 (2.00-4.00)	5.0 (4.00-5.00)	4.0 (2.00-5.00)

Table 2: The recognition rate (mean value w/ SD) and collected subjective responses with 7-point Likert scale (median value w/ interquartile range). The best ratings are in bold.

interaction [32]. We selected 100 ms as a stimulus duration and sinusoidal waveform with 160 Hz (resonant frequency found in **Technical Evaluation**) as a driving pattern. We mounted our prototypes on two different surfaces including a rigid acrylic plate and a soft silicone (EcoFlex^{TM} 00-10). We herein explored effect of mounting surface's mechanical hardness on users' tactile perception.

Results: Figure 9 shows the absolute threshold of sensation from each participant. The result verified that all thresholds were far below than occasionally observed *HapSense* dielectric breakdown voltage (> 400 V) which ensures the safety during device usage. Between the two mounting surfaces, we did not observe noticeable driving voltage threshold difference. From the result, it is recommended to keep the driving voltage at least above 150 V to deliver perceptible stimulation among broad range of different users with *HapSense*'s actuation.

Actuation Driving Waveform Investigation

We investigated the user's preference and performance (recognition rate) of vibrotactile actuation from *HapSense* which were driven at various waveforms. We investigated user perception of actuation when *HapSense* was in contact with Thumb, Index, multiple fingers, and Palm when *HapSense* was mounted either on a rigid surface or on a participant's wrist.

Since physical interaction with *HapSense* is executed mainly with hands, we narrowed our scope to hand regions as shown in Figure 10. We selected testing waveforms as shown in Table 2 including sine, square, and sawtooth waveform patterns with a peak voltage of 300 V at resonant frequencies measured in **Technical Evaluation**.

Setup: We selected four regions of hand consisting of different mechanoreceptor unit densities including thumb, index finger, multiple fingers, and palm [26] for the study. The duration and driving voltage of actuation was set to 2 s and 300 V accordingly. A 10 s pause was provided between trials. Also, we designed our study to incorporate 1) localization (*single* mode - actuating a single *HapSense* unit out of two neighbored units) and 2) spatiotemporal aspect (*dynamic* mode - actuating two adjacent *HapSense* units in sequence). We asked participants which unit had been actuated in *single* mode and the direction of actuation in *dynamic* mode.

For each set of trials, we asked participants about **sensitivity** ("*I could easily feel the vibration*"), **comfort** ("*This actuation is what I desired*"), and **discernibility** ("*It is easy to tell which area is vibrating*") of provided actuations using 7-point Likert scale similar to [44]. We collected subjective opinions to analyze preferable haptic parameters for *HapSense*.A total of 5184 data points (6 trials$\times$ 4 hand regions $\times$ 2 form factors $\times$ 2 modes $\times$ 6 haptic parameters $\times$ 9 users) and 864 subjective responses were collected.

Results: Table 2 shows that participants achieved the highest accuracy with the square wave and ranked it with the best sensitivity and discernibility. Participants reported having the highest comfort rating with a sine wave input. Participants commented that they felt a subtle and soft vibration with a sine wave whereas square & sawtooth waves were relatively easy to discern. Based on the results, we chose the square wave at a frequency of 160 Hz as a representative haptic parameter for **Main Study**.

MAIN STUDY

To further validate the functionality and explore design guidelines for *HapSense*, we targeted to answer the following questions: 1) How is the force sensing performance of proposed device on different operation modes and surfaces? 2) In *sensing-only* mode, what is the user-preferred input force to trigger an actuation event? These questions help us understand the basic functionality and the user preference while using *HapSense*.

In all evaluations, we used a prototype with 25 PVDF layers along with our board. For driving voltage waveform and frequency, we employed a square wave with 160 Hz which found out to be favorable sensation in **Exploratory Study**. We recruited 12 participants with a mean age of 29 (3 female). At the end of the study, we took a post survey for suggestions and applicable use case scenarios.

Task 1: HapSense Force Sensing Investigation

HapSense supports force sensing with two operation modes: *sensing-only* & *hybrid* modes. In this study, we investigated signal-to-noise ratio (SNR) on user's touch and press behavior for these two operation modes. Moreover, we carried out tests when *HapSense* device was mounted on a rigid acrylic plate and a participant's wrist to verify the effect of any potential sensing performance differences.

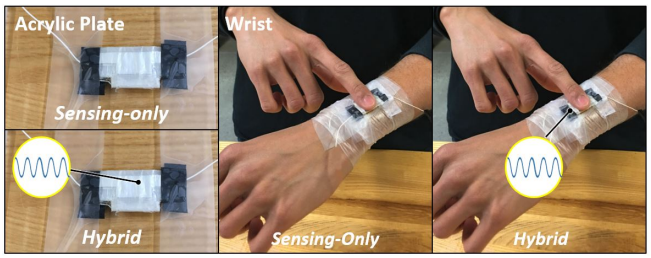

Figure 11: Study setup to measure SNR for two operation modes (*Sensing-only* & *Hybrid*) on different mounting surfaces (*Acrylic Plate* & *Wrist*).

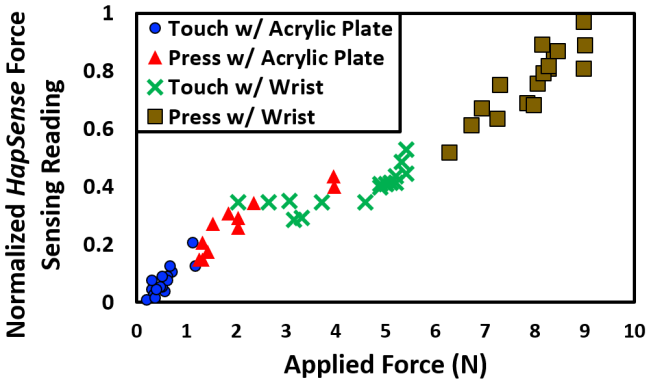

Figure 12: One exemplary force distribution pattern for "Touch" & "Press" behaviors (Multiple markers refer to representative data collected from different users).

Setup: We evaluated effects of two different *HapSense* mounting surfaces and operation modes as shown in Figure 11. We randomized the test parameter combination orders for different users to avoid learning effect. We asked participants to use their index finger to either *Touch* (similar force as general touch screen use as being elaborated in previous sections) or *Press* (user-defined force that can be differentiate from *Touch*). We measured the contact force from the participant on the acrylic plate and on the wrist using digital scale and a force sensitive resistor (FSR) sensor (FSR 402, Interlink Electronics), respectively. For *hybrid mode*, we used a driving voltage of 300 V with 160 Hz square wave as actuation driving parameters. For each condition, participants repeatedly (3 sets) performed 1*s* interval (20 data points) of *No Touch*, *Touch*, and *Press*. A total of 8640 data points were collected using our prototype (2 form factors $\times$ 2 operation modes $\times$ 3 tasks $\times$ 60 data points $\times$ 12 users). The SNR was calculated following the method discussed in [60].

Results: Figure 12 illustrates an exemplary distribution of *Touch* and *Press* from multiple participants with force sensing readings from *HapSense*. It is interesting to note that participants tend to apply larger forces for both *Touch* and *Press* when *HapSense* is mounted on a wrist comparing to on a rigid acrylic plate. This aligned with our observation where the participants showed a tendency to exert a fingertip contact until getting tactile sensations from the mounted body.

Figure 13 shows a force sensing SNR of *HapSense* with various parameters including mounting surfaces, operation modes, and contact behaviors. *HapSense* exhibits a relatively lower SNR when being on the wrist comparing to being placed on the acrylic plate. This can be explained by the electric field coupling between *HapSense* and the human body which is widely observed in capacitive sensors [4].

We also observed a lower force sensing SNR on *hybrid* mode comparing to *sensing-only* mode at the same conditions. We hypothesize this is due to electrical/mechanical noises from device actuation. Still, our results exhibit force sensing SNR higher than 23.5 *dB* [14], which is the minimum requirement for having robust touch sensing. This validates functionality of

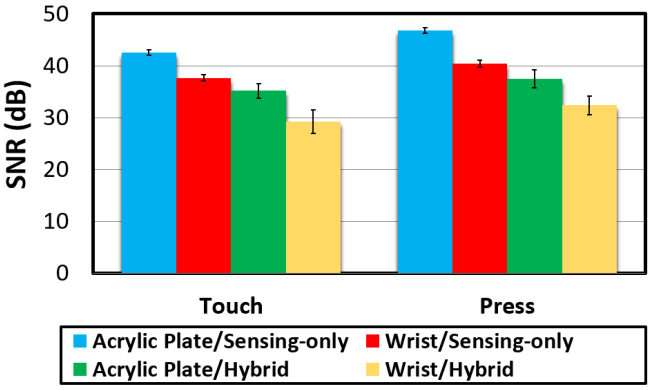

Figure 13: SNR with *HapSense* on two different mounting surfaces and operation modes.

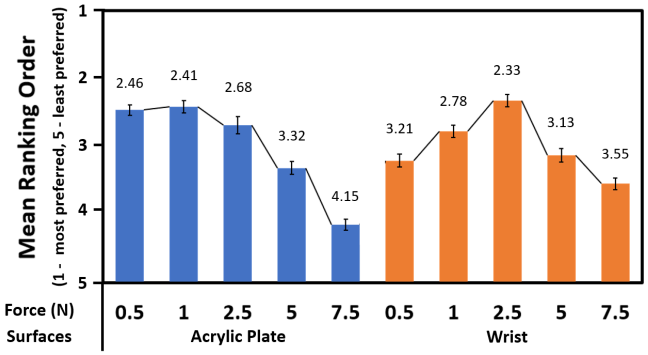

Figure 14: Mean ranking orders and S.E.M.s for the feedback stimuli. The ranking is arranged by triggering force threshold and surface type.

the force sensing with simultaneous actuation under different mounting surfaces and contact behaviors.

Task 2: HapSense Actuation Triggering Force

Previously, a study using rigid piezo ceramic buttons was carried out to identify user preference of vibration duration and time delay between user's touch input and actuator output [38]. In this study, we followed the reported ideal vibration duration (100 ms). We further extended the investigation scope using *HapSense*. To be more specific, we investigated the user preferred applied force to trigger *HapSense* actuation on different types of mounting surfaces including a rigid acrylic plate and participant's wrist. The study result will serve as a reference for operating soft haptic I/O on surfaces with different hardness.

Setup: We used the same hardware setup as described in Task 1, but without digital gauge and FSR sensor. For actuation driving waveform, we used a square wave with 160 Hz frequency, 300 V as peak voltage, and 100 ms as actuation duration. In our preliminary experiment, we found out a preferred contact force to trigger *HapSense* actuation ranged from 0.3 N to 10 N. Based on this observation, we set our triggering force levels as 0.5, 1, 2.5, 5, and 7.5 N. Since we directly use sensor reading to represent force values, *HapSense*'s sensor readings were fitted with digital gauge readings ($R^2 > 0.95$) prior to the study.

Participants were asked to rank among five different force triggering thresholds described above with five trials preceded by two practice trials. The participants were allowed to try and compare different thresholds as many time as they desired. The participants ranked from the most preferred pattern to the least preferred. In each trial, the sequence of five force thresholds was randomized. Following [38], we first analyzed with a Friedman test, then confirmed pairwise comparison with a Wilcoxon Signed Ranks test.

Results: In each trial, each triggering force threshold got a ranking score from 1 to 5 (1 = most preferred, 5 = least preferred). Figure 14 shows mean rankings and standard error of the means (S.E.M.s) of the feedback stimuli. The Friedman test showed a statistically significant effect of the feedback with $\chi^2 = 27.48$, $p < 0.01$. Wilcoxon Signed Ranks tests showed that *within Surfaces of*:

- *Acrylic Plate*, feedback with 0.5, 1, and 2.5, and 5 N triggering thresholds were rated significantly better than feedback with 7.5 N (Z = -2.10, $p < 0.05$, Z = -2.11, $p < 0.05$, Z = -1.97, $p < 0.05$, Z = -2.12, $p < 0.05$). 0.5 and 1N triggering thresholds were rated significantly better than feedback with 5 N (Z = -1.94, $p < 0.05$, Z = -2.01, $p < 0.05$).
- *Wrist*, feedback with 2.5 N triggering threshold was rated significantly better than feedback with 0.5, 5, and 7.5 N (Z = -2.13, $p < 0.05$, Z = -2.34, $p < 0.05$, Z = -2.34, $p < 0.05$). 1N triggering threshold was rated significantly better than 0.5 and 7.5N (Z = -2.04, $p < 0.05$, Z = -2.23, $p < 0.05$).

Based on the results, the participants showed preference on higher triggering force thresholds when using *HapSense* on the wrist. On the other hand, the light triggering force thresholds were preferred for interaction on a rigid surface. It is worth noting that the participants were not favored on the highest triggering force (7.5 N) on all surfaces. The results indicate that the triggering force threshold should be carefully selected according to applied mounting surfaces to ensure desired performance with *HapSense*.

Overall Feedback

We elicited qualitative user feedback on the overall *HapSense* experience. Participants favored the *HapSense*'s textured vibrotactile feedback and the comfort from soft/flexible material. Moreover, most participants were glad to find out that there existed no motors or rigid structures in the device. For improvements, participants recommended employing an aesthetic design and further making the device thinner while providing stronger actuation. Suggested application spaces include smart clothing, braille communication, VR controller, rehabilitation tool, and passive haptic training [56] tool.

EXAMPLE APPLICATIONS

We highlight a soft haptic I/O device that supports force sensing with integrated vibrotactile feedback. Comparing to previous works utilizing multiple hardware for sensing and actuation, the *HapSense* enable dual functionalities using only

a single device with uninterrupted system workflow and support applications which require thin and soft devices. The suggested examples showcase wide applicability of *HapSense*.

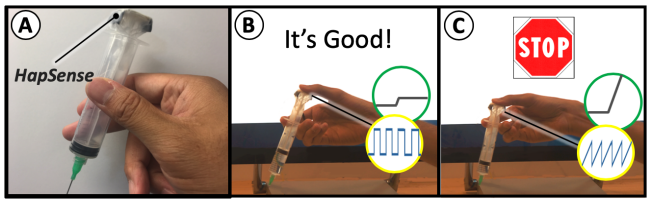

Figure 15: *HapSense* brings instructional guide for physical tool with integrated haptic feedback.

Haptic I/O Embedded Syringe for Training: *HapSense* can be attached to a syringe's plunger to train medical personnel controlling fluid injection rate (Figure 15). By sensing applied force on the plunger, vibrotactile actuation with distinctive waveforms can be provided to guide users' injection rate. This showcases a straightforward approach of making existing object as an interactive I/O device.

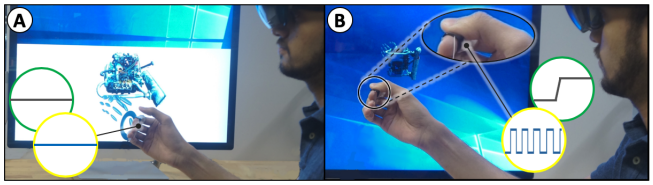

Figure 16: A wearable I/O sticker supports confident input.

Haptic I/O Sticker for VR: *HapSense* can be easily wrapped around or adhered onto human skin. *HapSense* vibrates when a user successfully executes a tap or press gesture to select 3D model in mixed reality environment. Users easily identify whether input control has been executed or not with integrated vibrotactile actuation. This demonstrates a potential in enhancing level of confidence during input commands for virtual environment.

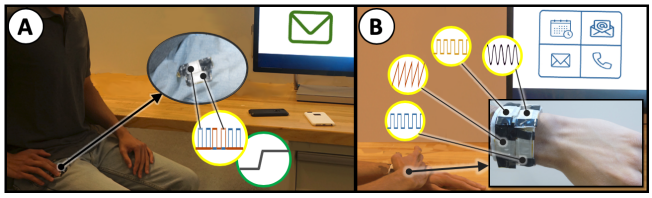

Figure 17: Supporting eyes-free & private interactions by embedding *HapSense* prototypes on (A) a pocket and (B) a wristband.

Interactive Wearables: Multiple *HapSense* are configured to support private and eyes-free interactions. Figure 17 (A) demonstrates using *HapSense* as a private haptic I/O device embedded onto clothing. For example, users naturally contact on pocket area to acquire different vibrotactile actuation patterns to decide if receiving messages from their smartphones. With assistance from *HapSense*, users do not have to look at the mobile device screen for checking notifications. Without needing of exposing personal device screen in public, to certain degree, we believe *HapSense* supports eyes-free as well as private interactions.

Figure 17 (B) illustrates a potential approach of providing rich localized feedback for eyes-free interaction. *HapSense* devices are attached to a fabric band to form a 2×2 interactive nodes. Each node can be customized to different software applications like *E-Mail*, *Messages*, *Calls* and *Calendar*. With a supported localized actuation from configured setup, users can acquire rich information without looking at the wearable device.

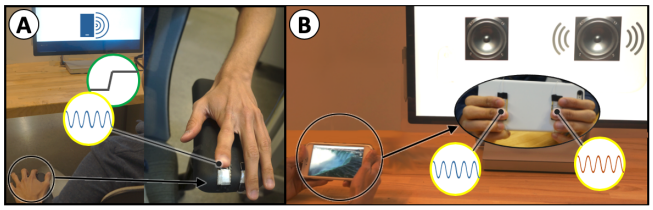

Figure 18: *HapSense* brings I/O functionalities as part of existing (A) rigid and (B) flexible objects with arbitrary shapes.

Armrest Haptic Controller: *HapSense* can be adapted on various mounting surfaces including uneven profiles. Multiple *HapSense* devices can be adhered to curved armrest as shown in Figure 18 (A). *HapSense* can easily turn the armrest into a controller with integrated vibrotactile feedback regardless its complicated external shape.

Interactive Phone Case: *HapSense* can be embedded onto various soft enclosures such as phone case with low-profile and soft form factor (Figure 18 (B)). The addition of soft I/O device onto phone case enables localized sensing and actuation on back of the device. Developing supported software (e.g., gaming, video streaming), *HapSense* shows great potential in enhancing user experience.

DISCUSSION

Durability & Structural Limitations: Currently, we have not conducted a comprehensive investigation to characterize system durability over large number of cycles. A rigid silver epoxy is currently applied for interconnection material between *HapSense* electrode and external circuitry. This limits the large bending deformation over the connection area. Potential remedies are to add durable protection layers or/and adopt more flexible/pliable conductive connections as silver epoxy alternatives. *HapSense* also needs to be evaluated in our future work with various environmental conditions (e.g., temperature, humidity, etc.).

Actuation Performance: The actuation resonant frequency of current prototype is not fully optimized for an effective skin-sensitive frequency range (200∼300 Hz) for human [39]. In future work, the resonant frequency profile of *HapSense* will be fully optimized by varying device's dimension/layer structure. Also, the current prototype is mainly designed to create tactile perception on user's fingertip rather than on the mounted body part (e.g., wrist). However, in our preliminary findings, when we deliberately enlarge HapSense active area

or enhance contact force between HapSense and wrist, it is achievable to enable actuation perception on user's wrist. This is currently under our active investigation. In addition, it is also within our interest to fully investigate specific application-driven performances (e.g., noticeability and discernibility) in the future.

Safety: Unlike electrostatic stimulation of skin, *HapSense* does not directly flow current to human skin and the output current at the high voltage rail is low (<10 μA). The electrodes are carefully sealed with insulated materials. Furthermore, the proposed custom hardware has a quick-discharging capability to ensure users safety.

Aesthetic Design: In current form factor, aesthetic design is not within our scope. To use *HapSense* as part of a practical consumer product, we will focus on improving its cosmetic appearance. Potential solutions would include employing cosmetic paints or cover materials.

Additional I/O Functionality: *HapSense* is capable of actuating at much higher frequency in audible frequency range, which has not been thoroughly investigated. This shows that *HapSense* has a potential in providing vibrotactile actuation, force sensing, as well as audio output which may result in broader application spaces.

PVDF is a ferroelectric polymer material. In this study, we utilized its piezoelectric physics. However, PVDF also shows pyroelectricity nature which has not been investigated in our current study. With pyroelectricity property, PVDF inherently induces electrical signals when experiencing environmental temperature change. It will potentially enable temperature variation as an additional input modality to *HapSense*.

CONCLUSION

We present a *HapSense*, a soft I/O device with uninterrupted dual functionalities of force sensing and vibrotactile actuation. We employ a multilayer ferroelectric electroactive polymer to achieve both input and output functionalities at reasonably low operating voltage as a soft device. We developed an advanced haptic system with novel hardware system workflow in a portable and miniaturized form factor. The electromechanical characterization validated the performance of *HapSense* as a sensor and an actuator. Throughout a series of user studies, we verified functionality and explored design guidelines to employ *HapSense*. We demonstrated example applications which showcase use of *HapSense* for meaningful and practical interactions. We envision to improve and expand interactions by bringing a soft I/O device in a highly integrated form factor.

REFERENCES

1. Brian P Bailey, Joseph A Konstan, and John V Carlis. 2001. The Effects of Interruptions on Task Performance, Annoyance, and Anxiety in the User Interface. In *Interact*, Vol. 1. 593–601.
2. Yoseph Bar-Cohen and others. 2004. *Electroactive polymer (EAP) actuators as artificial muscles: reality, potential, and challenges*. Vol. 5. SPIE press Bellingham, WA. https://doi.org/10.1117/3.547465.ch21
3. Olivier Bau and Ivan Poupyrev. 2012. REVEL: tactile feedback technology for augmented reality. *ACM Transactions on Graphics (TOG)* 31, 4 (2012), 89. https://doi.acm.org/10.1145/2185520.2185585
4. Larry K Baxter. 1997. *Capacitive Sensors: Design and Applications*. https://doi.org/10.1109/9780470544228
5. Frank Beruscha, Wolfgang Krautter, Yong Heng So, and Jin Han Jeon. 2018. It's a PHAct: Printed Haptic Actuators for Augmented Objects and Surfaces. In *Proceedings of the 2018 ACM International Joint Conference and 2018 International Symposium on Pervasive and Ubiquitous Computing and Wearable Computers*. ACM, 9–12. https://doi.org/10.1145/3267305.3267617
6. Frank Biocca, Arthur Tang, Charles Owen, and Fan Xiao. 2006. Attention funnel: omnidirectional 3D cursor for mobile augmented reality platforms. In *Proceedings of the SIGCHI conference on Human Factors in computing systems*. ACM, 1115–1122.
7. Alberto Boem and Giovanni Maria Troiano. 2019. Non-Rigid HCI: A Review of Deformable Interfaces and Input. In *Proceedings of the 2019 on Designing Interactive Systems Conference (DIS '19)*. ACM, New York, NY, USA, 885–906. DOI: http://dx.doi.org/10.1145/3322276.3322347
8. Stephen Brewster. 2002. Overcoming the lack of screen space on mobile computers. *Personal and Ubiquitous Computing* 6, 3 (2002), 188–205. https://doi.org/10.1007/s007790200019
9. Dustin Chen and Qibing Pei. 2017. Electronic muscles and skins: A review of soft sensors and actuators. *Chemical reviews* 117, 17 (2017), 11239–11268. https://doi.org/10.1021/acs.chemrev.7b00019
10. Seungmoon Choi and Katherine J Kuchenbecker. 2013. Vibrotactile display: Perception, technology, and applications. *Proc. IEEE* 101, 9 (2013), 2093–2104. https://doi.org/10.1109/jproc.2012.2221071
11. Alex Chortos, Jia Liu, and Zhenan Bao. 2016. Pursuing prosthetic electronic skin. *Nature materials* 15, 9 (2016), 937. https://doi.org/10.1038/nmat4671
12. Nguyen Huu Chuc, Doan Vu Thuy, Jonggil Park, Duksang Kim, Jachoon Koo, Youngkwan Lee, Jae-Do Nam, and Hyouk Ryeol Choi. 2008. A dielectric elastomer actuator with self-sensing capability. In *Electroactive Polymer Actuators and Devices (EAPAD)*,

Vol. 6927. International Society for Optics and Photonics. https://doi.org/10.1117/12.776831

13. Tom N Cornsweet. 1962. The staircrase-method in psychophysics. *The American Journal of Psychology* 75, 3 (1962), 485–491. https://10.2307/1419876
14. Burke Davison. 2010. Techniques for robust touch sensing design. *AN1334 Microchip Technology Inc* (2010), 53.
15. Sean Follmer, Daniel Leithinger, Alex Olwal, Akimitsu Hogge, and Hiroshi Ishii. 2013. inFORM: dynamic physical affordances and constraints through shape and object actuation.. In *Proceedings of the 26th Annual Symposium on User Interface Software and Technology*, Vol. 13. 417–426. https://doi.org/10.1145/2501988.2502032
16. Karmen Franinović and Luke Franzke. 2019. Shape Changing Surfaces and Structures: Design Tools and Methods for Electroactive Polymers. In *Proceedings of the 2019 CHI Conference on Human Factors in Computing Systems*. ACM, 125. https://doi.org/10.1145/3290605.3300355
17. Christian Frisson, Julien Decaudin, Thomas Pietrzak, Alexander Ng, Pauline Poncet, Fabrice Casset, Antoine Latour, and Stephen A Brewster. 2017. Designing Vibrotactile Widgets with Printed Actuators and Sensors. In *Adjunct Publication of the 30th Annual ACM Symposium on User Interface Software and Technology*. ACM, 11–13. https://doi.org/10.1145/3131785.3131800
18. George A Gescheider. 1997. *Psychophysics: the fundamentals*. Psychology Press. https://doi.org/10.4324/9780203774458
19. Guo-Ying Gu, Jian Zhu, Li-Min Zhu, and Xiangyang Zhu. 2017. A survey on dielectric elastomer actuators for soft robots. *Bioinspiration & biomimetics* 12, 1 (2017), 011003. https://doi.org/10.1088/1748-3190/12/1/011003
20. Carter S Haines, Márcio D Lima, Na Li, Geoffrey M Spinks, Javad Foroughi, John DW Madden, Shi Hyeong Kim, Shaoli Fang, Mônica Jung de Andrade, Fatma Göktepe, and others. 2014. Artificial muscles from fishing line and sewing thread. *science* 343, 6173 (2014), 868–872. https://doi.org/10.1126/science.1246906
21. Kelly S Hale and Kay M Stanney. 2004. Deriving haptic design guidelines from human physiological, psychophysical, and neurological foundations. *IEEE computer graphics and applications* 24, 2 (2004), 33–39. https://doi.org/10.1109/MCG.2004.1274059
22. Nur Al-huda Hamdan, Adrian Wagner, Simon Voelker, Jürgen Steimle, and Jan Borchers. 2019. Springlets: Expressive, Flexible and Silent On-Skin Tactile Interfaces. In *Proceedings of the 2019 CHI Conference on Human Factors in Computing Systems (CHI '19)*. ACM, New York, NY, USA, Article 488, 14 pages. DOI: http://dx.doi.org/10.1145/3290605.3300718
23. Eve Hoggan, Stephen A Brewster, and Jody Johnston. 2008. Investigating the effectiveness of tactile feedback for mobile touchscreens. In *Proceedings of the SIGCHI conference on Human factors in computing systems*. ACM, 1573–1582. https://doi.org/10.1145/1357054.1357300
24. Texas Instrument. 2019. DRV2667. (2019). Retrieved July 1, 2019 from https://www.ti.com.
25. Yvonne Jansen, Thorsten Karrer, and Jan Borchers. 2010. MudPad: tactile feedback and haptic texture overlay for touch surfaces. In *ACM International Conference on Interactive Tabletops and Surfaces*. ACM, 11–14. https://doi.org/10.1145/1936652.1936655
26. Roland S Johansson and AB Vallbo. 1979. Tactile sensibility in the human hand: relative and absolute densities of four types of mechanoreceptive units in glabrous skin. *The Journal of physiology* 286, 1 (1979), 283–300. https://doi.org/10.1113/jphysiol.1979.sp012619
27. Jingun Jung, Eunhye Youn, and Geehyuk Lee. 2017. PinPad: touchpad interaction with fast and high-resolution tactile output. In *Proceedings of the 2017 CHI Conference on Human Factors in Computing Systems*. ACM, 2416–2425.
28. Kwangmok Jung, Kwang J Kim, and Hyouk Ryeol Choi. 2008. A self-sensing dielectric elastomer actuator. *Sensors and Actuators A: Physical* 143, 2 (2008), 343–351. https://doi.org/10.1016/j.sna.2007.10.076
29. Kurt A Kaczmarek, John G Webster, Paul Bach-y Rita, and Willis J Tompkins. 1991. Electrotactile and vibrotactile displays for sensory substitution systems. *IEEE Transactions on Biomedical Engineering* 38, 1 (1991), 1–16. https://doi.org/10.1109/10.68204
30. Hsin-Liu Cindy Kao, Christian Holz, Asta Roseway, Andres Calvo, and Chris Schmandt. 2016. DuoSkin: Rapidly prototyping on-skin user interfaces using skin-friendly materials. In *Proceedings of the 2016 ACM International Symposium on Wearable Computers*. ACM, 16–23. https://doi.org/10.1145/2971763.2971777
31. Akito Kawamata, Yoichi Kadota, Hiroshi Hosaka, and Takeshi Morita. 2008. Self-sensing piezoelectric actuator using permittivity detection. *Ferroelectrics* 368, 1 (2008), 194–201. https://doi.org/10.1080/00150190802368495
32. Jeong Ho Kim, Lovenoor Aulck, Michael C Bartha, Christy A Harper, and Peter W Johnson. 2012. Are there differences in force exposures and typing productivity between touchscreen and conventional keyboard?. In *Proceedings of the Human Factors and Ergonomics Society Annual Meeting*, Vol. 56. SAGE Publications Sage CA: Los Angeles, CA, 1104–1108. https://doi.org/10.1177/1071181312561240
33. Michinari Kono, Takumi Takahashi, Hiromi Nakamura, Takashi Miyaki, and Jun Rekimoto. 2018. Design Guideline for Developing Safe Systems that Apply Electricity to the Human Body. *ACM Transactions on Computer-Human Interaction (TOCHI)* 25, 3 (2018), 19. https://doi.org/10.1145/3184743

34. Ig Mo Koo, Kwangmok Jung, Ja Choon Koo, Jae-Do Nam, Young Kwan Lee, and Hyouk Ryeol Choi. 2008. Development of soft-actuator-based wearable tactile display. *IEEE Transactions on Robotics* 24, 3 (2008), 549–558. https://doi.org/10.1109/tro.2008.921561

35. Karl Kruusamäe, Andres Punning, Alvo Aabloo, and Kinji Asaka. 2015. Self-sensing ionic polymer actuators: a review. (2015). https://doi.org/10.3390/act4010017

36. Ki-Uk Kyung and Jun-Young Lee. 2009. Ubi-Pen: a haptic interface with texture and vibrotactile display. *IEEE Computer Graphics and Applications* 29, 1 (2009). https://doi.org/10.1109/mcg.2009.17

37. Johnny C Lee, Paul H Dietz, Darren Leigh, William S Yerazunis, and Scott E Hudson. 2004. Haptic pen: a tactile feedback stylus for touch screens. In *Proceedings of the 17th annual ACM symposium on User interface software and technology*. ACM, 291–294. https://doi.org/10.1145/1029632.1029682

38. Jani Lylykangas, Veikko Surakka, Katri Salminen, Jukka Raisamo, Pauli Laitinen, Kasper Rönning, and Roope Raisamo. 2011. Designing tactile feedback for piezo buttons. In *Proceedings of the SIGCHI Conference on Human Factors in Computing Systems*. ACM, 3281–3284. https://doi.org/10.1145/1978942.1979428

39. Takashi Maeno. 2000. Structure and function of finger pad and tactile receptors. *Journal of the Robotics Society of Japan* 18, 6 (2000), 772–775. https://doi.org/10.7210/jrsj.18.772

40. Tissaphern Mirfakhrai, John DW Madden, and Ray H Baughman. 2007. Polymer artificial muscles. *Materials today* 10, 4 (2007), 30–38. https://doi.org/10.1016/S1369-7021(07)70048-2

41. Viktor Miruchna, Robert Walter, David Lindlbauer, Maren Lehmann, Regine Von Klitzing, and Jörg Müller. 2015. GelTouch: Localized Tactile Feedback Through Thin, Programmable Gel. In *Proceedings of the 28th Annual ACM Symposium on User Interface Software & Technology*. ACM, 3–10. https://doi.org/10.1145/2807442.2807487

42. Yong-Lae Park, Bor-Rong Chen, and Robert J Wood. 2012. Design and fabrication of soft artificial skin using embedded microchannels and liquid conductors. *IEEE Sensors Journal* 12, 8 (2012), 2711–2718. https://doi.org/10.1109/JSEN.2012.2200790

43. Jerome Pasquero, Scott J Stobbe, and Noel Stonehouse. 2011. A haptic wristwatch for eyes-free interactions. In *Proceedings of the SIGCHI Conference on Human Factors in Computing Systems*. ACM, 3257–3266. https://doi.org/10.1145/1978942.1979425

44. Fabrizio Pece, Juan Jose Zarate, Velko Vechev, Nadine Besse, Olexandr Gudozhnik, Herbert Shea, and Otmar Hilliges. 2017. MagTics: Flexible and Thin Form Factor Magnetic Actuators for Dynamic and Wearable Haptic Feedback. In *Proceedings of the 30th annual ACM symposium on User interface software and technology*. ACM, 143–154. https://doi.org/10.1145/3126594.3126609

45. Simon T Perrault, Eric Lecolinet, James Eagan, and Yves Guiard. 2013. Watchit: Simple Gestures and Eyes-free Interaction for Wristwatches and Bracelets. In *Proceedings of the SIGCHI Conference on Human Factors in Computing Systems*. ACM, 1451–1460. https://doi.org/10.1145/2470654.2466192

46. Piezotech. 2019. Piezotech polymers. (2019). Retrieved July 1, 2019 from https://www.piezotech.eu.

47. Pauline Poncet, Fabrice Casset, Antoine Latour, F Domingues Dos Santos, Sébastien Pawlak, Romain Gwoziecki, and Stéphane Fanget. 2016. Design and realization of electroactive polymer actuators for transparent and flexible haptic feedback interfaces. In *2016 17th International Conference on Thermal, Mechanical and Multi-Physics Simulation and Experiments in Microelectronics and Microsystems (EuroSimE)*. IEEE, 1–5. https://doi.org/10.1109/eurosime.2016.7463310

48. Ivan Poupyrev, Tatsushi Nashida, and Makoto Okabe. 2007. Actuation and tangible user interfaces: the Vaucanson duck, robots, and shape displays. In *Proceedings of the 1st international conference on Tangible and embedded interaction*. ACM, 205–212. https://doi.org/10.1145/1226969.1227012

49. Jun Rekimoto and Carsten Schwesig. 2006. PreSenseII: Bi-directional Touch and Pressure Sensing Interactions with Tactile Feedback. In *CHI'06 extended abstracts on Human factors in computing systems*. ACM, 1253–1258. https://doi.org/10.1145/1125451.1125685

50. Hendrik Richter, Ronald Ecker, Christopher Deisler, and Andreas Butz. 2010. HapTouch and the 2+1 state model: potentials of haptic feedback on touch based in-vehicle information systems. In *Proceedings of the 2nd international conference on automotive user interfaces and interactive vehicular applications*. ACM, 72–79. https://doi.org/10.1145/1969773.1969787

51. Gianluca Rizzello, Federica Fugaro, David Naso, and Stefan Seelecke. 2018. Simultaneous Self-Sensing of Displacement and Force for Soft Dielectric Elastomer Actuators. *IEEE Robotics and Automation Letters* 3, 2 (2018), 1230–1236. https://doi.org/10.1109/lra.2018.2795016

52. Simon Robinson, Céline Coutrix, Jennifer Pearson, Juan Rosso, Matheus Fernandes Torquato, Laurence Nigay, and Matt Jones. 2016. Emergeables: Deformable displays for continuous eyes-free mobile interaction. In *Proceedings of the 2016 CHI Conference on Human Factors in Computing Systems*. ACM, 3793–3805. https://doi.org/10.1145/2858036.2858097

53. Samuel Rosset, Oluwaseun A Araromi, Samuel Schlatter, and Herbert R Shea. 2016. Fabrication process of silicone-based dielectric elastomer actuators. *JoVE (Journal of Visualized Experiments)* 108 (2016), e53423. https://doi.org/10.3791/53423

54. Samuel Rosset, Benjamin M OâĂŹBrien, Todd Gisby, Daniel Xu, Herbert R Shea, and Iain A Anderson. 2013. Self-sensing dielectric elastomer actuators in closed-loop operation. *Smart Materials and Structures* 22, 10 (2013), 104018. https://doi.org/10.1088/0964-1726/22/10/104018

55. Anne Roudaut, Andreas Rau, Christoph Sterz, Max Plauth, Pedro Lopes, and Patrick Baudisch. 2013. Gesture Output: Eyes-free Output using a Force Feedback Touch Surface. In *Proceedings of the SIGCHI Conference on Human Factors in Computing Systems*. ACM, 2547–2556. https://doi.org/10.1145/2470654.2481352

56. Caitlyn Seim, Nick Doering, Yang Zhang, Wolfgang Stuerzlinger, and Thad Starner. 2017. Passive Haptic Training to Improve Speed and Performance on a Keypad. *Proceedings of the ACM on Interactive, Mobile, Wearable and Ubiquitous Technologies* 1, 3 (2017), 100. https://doi.org/10.1145/3132026

57. Harshal Arun Sonar and Jamie Paik. 2016. Soft pneumatic actuator skin with piezoelectric sensors for vibrotactile feedback. *Frontiers in Robotics and AI* 2 (2016), 38. https://doi.org/10.3389/frobt.2015.00038

58. Saeedeh Ebrahimi Takalloo, Hasti Seifi, and John DW Madden. 2017. Design of ultra-thin high frequency trilayer conducting polymer micro-actuators for tactile feedback interfaces. In *Electroactive Polymer Actuators and Devices (EAPAD) 2017*, Vol. 10163. International Society for Optics and Photonics. https://doi.org/10.1117/12.2262269

59. TDK. 2019. PiezoHapt Ultra-Thin Actuators. (2019). Retrieved July 1, 2019 from https://www.mouser.com/new/tdk/tdk-piezo-hapt-actuator.

60. Schnoor Walter. 2018. Sensitivity, SNR, and Design Margin in Capacitive Touch Applications. *Application Report* (2018).

61. Martin Weigel, Tong Lu, Gilles Bailly, Antti Oulasvirta, Carmel Majidi, and Jürgen Steimle. 2015. iSkin: Flexible, Stretchable and Visually Customizable On-Body Touch Sensors for Mobile Computing. In *Proceedings of the 33rd Annual ACM Conference on Human Factors in Computing Systems*. ACM, 2991–3000. https://doi.org/10.1145/2702123.2702391

62. Michael Wessely, Theophanis Tsandilas, and Wendy E Mackay. 2016. Stretchis: Fabricating Highly Stretchable User Interfaces. In *Proceedings of the 29th Annual Symposium on User Interface Software and Technology*. ACM, 697–704. https://doi.org/10.1145/2984511.2984521

63. Anusha Withana, Daniel Groeger, and JÃijrgen Steimle. 2018. Tacttoo: A Thin and Feel-Through Tattoofor On-Skin Tactile Output. In *Proceedings of the 30th Annual ACM Symposium on User Interface Software and Technology*. ACM, To Appear. https://doi.org/10.1145/3242587.3242645

64. Lining Yao, Ryuma Niiyama, Jifei Ou, Sean Follmer, Clark Della Silva, and Hiroshi Ishii. 2013. PneUI: Pneumatically Actuated Soft Composite Materials for Shape Changing Interfaces. In *Proceedings of the 26th annual ACM symposium on User interface software and Technology*. ACM, 13–22. https://doi.org/10.1145/2501988.2502037

65. Sang Ho Yoon, Ke Huo, Yunbo Zhang, Guiming Chen, Luis Paredes, Subramanian Chidambaram, and Karthik Ramani. 2017. iSoft: A Customizable Soft Sensor with Real-time Continuous Contact and Stretching Sensing. In *Proceedings of the 30th Annual ACM Symposium on User Interface Software and Technology*. ACM, 665–678. https://doi.org/10.1145/3126594.3126654